

## Physical properties of $\text{InF}_3$ -based glasses

JOANNA PISARSKA<sup>1</sup>, MARIA ŚLĘZOK<sup>1</sup>, MICHAŁ ŻELECHOWER<sup>1</sup>, WOJCIECH A. PISARSKI<sup>2</sup>, TOMASZ GORYCZKA<sup>2</sup>, WITOLD RYBA-ROMANOWSKI<sup>3</sup>

<sup>1</sup>Silesian University of Technology, Department of Materials Science, ul. Zygmunta Krasińskiego 8, 40–019 Katowice, Poland.

<sup>2</sup>University of Silesia, Institute of Physics and Chemistry of Metals, ul. Bankowa 12, 40–007 Katowice, Poland.

<sup>3</sup>Institute of Low Temperature and Structure Research, Polish Academy of Sciences, ul. Okólna 2, 50–395 Wrocław, Poland.

Results of X-ray diffraction (XRD), differential scanning calorimetry (DSC), electron probe microanalysis (EPMA) and optical absorption of  $\text{InF}_3$ -based glasses are reported. Different concentrations of rare earth ions have been added to a base glass. XRD results show that no crystalline phases are formed. Characteristic temperatures were determined by DSC and values of glass stability parameters were calculated. Also, the effect of rare earth ions on the thermal stability of  $\text{InF}_3$ -based glasses has been investigated. From the optical absorption measurements and Judd–Ofelt method the intensity parameters have been calculated. In consequence the trends of the intensity parameters are discussed as a function of the number of  $4f$  electrons.

Keywords: fluorindate glasses, rare earth fluoride, physical properties.

### 1. Introduction

Heavy metal fluoride glasses (HMFG) have been studied extensively in recent years [1]–[5]. In particular, glasses based on indium fluoride have drawn attention because of their attractive optical properties such as lower phonon energy, wide IR transmission range, as well as higher thermal stability in the other ones. Recently, the optical properties of  $\text{InF}_3$ – $\text{ZnF}_2$ – $\text{BaF}_2$ – $\text{SrF}_2$ – $\text{GaF}_3$ – $\text{NaF}$  (IZBSGN) systems singly doped with  $\text{Tm}^{3+}$  and doubly doped with  $\text{Tm}^{3+}$  and  $\text{Tb}^{3+}$  ions have been investigated [6]. In this paper, we provide some information about thermal and optical properties of  $\text{InF}_3$ -based glasses doped with different concentrations of rare earth fluorides. The detailed knowledge about how do these properties change as a function of the modifiers addition and the rare earth doping to the base glass is crucial in the evaluation of a glass matrix as a laser media host or optical waveguide.

## 2. Experimental

X-ray diffraction (XRD) patterns of glass samples were obtained using INEL diffractometer with Cu  $K_\alpha$  radiation in  $2\theta$  range from  $0^\circ$  to  $120^\circ$ . Homogeneity measurements (EPMA) were performed using scanning electron microscope (JSM 35) coupled with an energy dispersion X-ray spectrometer (LINK 860). Characteristic temperatures were determined from a differential scanning calorimetry (DSC) analysis (Perkin–Elmer). Optical absorption spectra were recorded with a Varian 2300 UV-VIS-NIR spectrophotometer.

## 3. Results and discussion

### 3.1. Synthesis and characterization of $\text{InF}_3$ -based systems

Several glass matrices of nominal compositions (in mol%):  $40\text{InF}_3\text{-}20\text{ZnF}_2\text{-}20\text{BaF}_2\text{-}20\text{SrF}_2$  (IZBS) and  $36\text{InF}_3\text{-}20\text{ZnF}_2\text{-}16\text{BaF}_2\text{-}20\text{SrF}_2\text{-}6\text{GaF}_3\text{-}2\text{NaF}$  (IZBSGN) were prepared using anhydrous fluorides of 99.99% purity (Aldrich) as starting materials. In doped samples the  $\text{InF}_3$  was substituted partially in order to obtain systems singly doped with 2% and 8% of  $\text{Eu}^{3+}$ , 0.5% and 6% of  $\text{Ho}^{3+}$ , 0.5% and 5% of  $\text{Tm}^{3+}$ . To prepare samples, several batches were mixed homogeneously and heated in dry argon atmosphere. Glasses were melted at  $850^\circ\text{C}$  in a platinum crucible, then poured into preheated copper moulds and annealed below the glass transition temperature  $T_g$ . After this process, samples were slowly cooled to the room temperature. Some of the physical properties including: characteristic temperatures, stability parameter and refractive index of undoped IZBS and IZBSGN glasses, in comparison to other glasses based on  $\text{InF}_3$ , are presented in Tab. 1. Different  $T_g$  and  $\Delta T$  values are observed for our IZBS glass and glass with the same composition but obtained by other co-workers. This discrepancy probably can be associated with different conditions in which the samples were prepared. The stability parameter  $\Delta T$  increases when glass-modifiers such as  $\text{GaF}_3$  and  $\text{NaF}$  substitute for  $\text{InF}_3$  and  $\text{BaF}_2$ . In the presence of these modifiers the stability parameter  $\Delta T$  is higher than for IZBS and other glasses well described in literature.

### 3.2. XRD and EPMA studies

The preliminary X-ray diffraction analysis of  $\text{InF}_3$ -based glasses (IZBSGN) doped with rare earth ions was carried out. Figure 1 shows the X-ray diffraction patterns obtained for glasses doped with  $\text{Eu}^{3+}$ ,  $\text{Ho}^{3+}$ ,  $\text{Tm}^{3+}$  ions. The XRD patterns of our glasses display two broad peaks corresponding to the remaining amorphous phases, independently of rare earth doping concentration. The same behavior is observed in the case of an undoped sample. In contrast to other  $\text{InF}_3$ -based glasses these findings are in a good agreement with the results obtained for IZBSGa and IZBSMg after heat treatment, where no crystalline phase was detected [2]. In order to obtain additional information on the crystallizing phases, X-ray diffraction measurements should be performed after the heat treatment. EPMA measurements indicate a good chemical

Table 1. Physical characteristics of glasses in the  $\text{InF}_3$ -based system. Characteristic temperatures  $T_g$  and  $T_x$ , stability parameter  $\Delta T$  and refractive index  $n_D$  from this study compared with other heavy metal fluoride glasses based on indium fluoride.

Sample	Composition [mol%]	$n_D$	$T_g$ [°C]	$T_x$ [°C]	$\Delta T$ [°C]	Ref.
IZBS	40 $\text{InF}_3$ -20 $\text{ZnF}_2$ -20 $\text{BaF}_2$ -20 $\text{SrF}_2$	1.501	301	388	87	[1]
IZBSNa	36 $\text{InF}_3$ -30 $\text{ZnF}_2$ -15 $\text{BaF}_2$ -20 $\text{SrF}_2$ -4 $\text{NaF}$	—	307	370	63	[2]
IZSBNa	30 $\text{InF}_3$ -30 $\text{ZnF}_2$ -15 $\text{BaF}_2$ -20 $\text{SrF}_2$ -5 $\text{NaF}$	1.487	290	380	90	[3]
IZBGdCa	40 $\text{InF}_3$ -20 $\text{ZnF}_2$ -25 $\text{BaF}_2$ -10 $\text{GdF}_3$ -5 $\text{CaF}_2$	—	309	403.6	94.6	[4]
IZBGdCaY	46 $\text{InF}_3$ -20 $\text{ZnF}_2$ -30 $\text{BaF}_2$ -2 $\text{GdF}_3$ -5 $\text{CaF}_2$ -2 $\text{YF}_3$	—	303	278.9	75.9	[4]
IZBSCa	36 $\text{InF}_3$ -30 $\text{ZnF}_2$ -15 $\text{BaF}_2$ -20 $\text{SrF}_2$ -4 $\text{CaF}_2$	—	302	375	73	[2]
IZSBC	40 $\text{InF}_3$ -20 $\text{ZnF}_2$ -15 $\text{BaF}_2$ -20 $\text{SrF}_2$ -5 $\text{CaF}_2$	1.495	295	385	90	[3]
IZBSCd	36 $\text{InF}_3$ -20 $\text{ZnF}_2$ -20 $\text{BaF}_2$ -20 $\text{SrF}_2$ -4 $\text{CdF}_2$	—	301	390	89	[2]
IZSBCd	40 $\text{InF}_3$ -20 $\text{ZnF}_2$ -15 $\text{BaF}_2$ -20 $\text{SrF}_2$ -5 $\text{CdF}_2$	1.498	291	383	92	[3]
IZSBPb	40 $\text{InF}_3$ -20 $\text{ZnF}_2$ -25 $\text{BaF}_2$ -5 $\text{SrF}_2$ -10 $\text{PbF}_2$	1.530	277	366	89	[3]
IZBSMg	36 $\text{InF}_3$ -20 $\text{ZnF}_2$ -20 $\text{BaF}_2$ -20 $\text{SrF}_2$ -4 $\text{MgF}_2$	—	311	405	94	[2]
IZBSGa	36 $\text{InF}_3$ -20 $\text{ZnF}_2$ -20 $\text{BaF}_2$ -20 $\text{SrF}_2$ -4 $\text{GaF}_3$	—	309	414	105	[2]
IZBSY	36 $\text{InF}_3$ -20 $\text{ZnF}_2$ -20 $\text{BaF}_2$ -20 $\text{SrF}_2$ -4 $\text{YF}_3$	—	309	395	86	[2]
IZBSZr	36 $\text{InF}_3$ -20 $\text{ZnF}_2$ -20 $\text{BaF}_2$ -20 $\text{SrF}_2$ -4 $\text{ZrF}_4$	—	306	391	85	[2]
IZBGd	40 $\text{InF}_3$ -20 $\text{ZnF}_2$ -30 $\text{BaF}_2$ -10 $\text{GdF}_3$	—	309	392.2	83.2	[4]
IZBGdAl	40 $\text{InF}_3$ -20 $\text{ZnF}_2$ -25 $\text{BaF}_2$ -10 $\text{GdF}_3$ -5 $\text{AlF}_3$	—	310.7	400	89.3	[4]
IZBGdSr	40 $\text{InF}_3$ -20 $\text{ZnF}_2$ -20 $\text{BaF}_2$ -10 $\text{GdF}_3$ -10 $\text{SrF}_2$	—	300	405	105	[4]
IZBSGd	36 $\text{InF}_3$ -20 $\text{ZnF}_2$ -20 $\text{BaF}_2$ -20 $\text{SrF}_2$ -4 $\text{GdF}_3$	—	317	360	43	[2]
IZBSGdNa	40 $\text{InF}_3$ -20 $\text{ZnF}_2$ -15 $\text{BaF}_2$ -20 $\text{SrF}_2$ -3 $\text{GdF}_3$ -2 $\text{NaF}$	1.498	291	383	92	[5]
IZSBGdNa	40 $\text{InF}_3$ -20 $\text{ZnF}_2$ -16 $\text{BaF}_2$ -20 $\text{SrF}_2$ -2 $\text{GdF}_3$ -2 $\text{NaF}$	1.493	289	390	101	[3]
IZSBGdL	40 $\text{InF}_3$ -20 $\text{ZnF}_2$ -17 $\text{BaF}_2$ -20 $\text{SrF}_2$ -2 $\text{GdF}_3$ -1 $\text{LaF}_3$	1.508	294	390	96	[3]
IZBS	40 $\text{InF}_3$ -20 $\text{ZnF}_2$ -20 $\text{BaF}_2$ -20 $\text{SrF}_2$	—	292	392	100	
IZBSGN	36 $\text{InF}_3$ -20 $\text{ZnF}_2$ -16 $\text{BaF}_2$ -20 $\text{SrF}_2$ -6 $\text{GaF}_3$ -2 $\text{NaF}$	1.48	294	404	110	

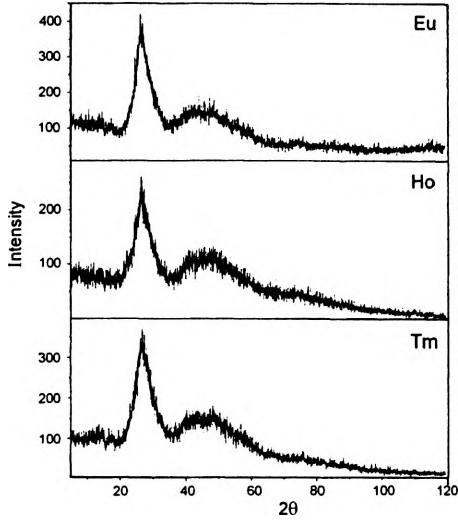


Fig. 1. X-ray diffraction patterns of  $\text{InF}_3$ -based glasses doped with  $\text{Eu}^{3+}$ ,  $\text{Ho}^{3+}$  and  $\text{Tm}^{3+}$  ions.

T a b l e 2. Results of elemental homogeneity measurements.

IZBSGNEu 8 mol% Eu	In	Ba	Eu	Zn	Ga	Sr
Average intensity [counts]	8530	3696	672	3898	803	846
Standard deviation [counts]	266	93	148	238	51	50
Relative mean error [%]	1.4	1.1	9.9	2.7	2.8	2.7
IZBSGNEu 2 mol% Eu			Eu			
Average intensity [counts]		8375	3678			2154
Standard deviation [counts]		526.4	371.8			131.7
Relative mean error [%]		2.0	3.2			1.9
IZBSGNTm 0.5 mol% Tm	In	Ba	Tm	Zn	Ga	Sr
Average intensity [counts]	11315	4440	152	4045	195	714
Standard deviation [counts]	283	46	32	72	52	34
Relative mean error [%]	1.1	0.5	9.4	0.8	12.0	2.1
IZBSGNTm 5 mol% Tm			Tm			
Average intensity [counts]		11420	2179			2555
Standard deviation [counts]		265.5	147.9			160.2
Relative mean error [%]		0.7	2.1			2.0
IZBSGNHo 0.5 mol% Ho	In	Ba	Ho	Zn	Ga	Sr
Average intensity [counts]	9989	10040	1201	3910	775	2221
Standard deviation [counts]	271	278.2	80.9	197	50	81.3
Relative mean error [%]	1.2	0.9	2.1	2.5	2.7	1.2
IZBSGNHo 6 mol% Ho			Ho			
Average intensity [counts]		10925	5737			2360
Standard deviation [counts]		844.6	846.5			257.8
Relative mean error [%]		2.4	4.7			3.5

homogeneity of our glasses. Results of homogeneity measurements are presented in Tab. 2. In most cases, for elements with a high concentration the relative mean error does not exceed 3%, however, for elements with a low concentration (Ga, rare earth) it reaches the value close to 10%.

### 3.3. DSC study

From DSC curves characteristic temperatures such as glass transition temperature  $T_g$ , crystallization onset  $T_x$  and maximum of the crystallization peak  $T_p$  were obtained, from which stability parameter  $\Delta T$  was calculated for undoped IZBS and IZBSGN glasses, as well as for both glasses doped with 2 mol% of  $\text{Eu}^{3+}$ . As mentioned in Sec. 3.1, the stability parameter  $\Delta T$  increases from 100 °C for IZBS up to 110 °C for IZBSGN with the addition of  $\text{GaF}_3$  and  $\text{NaF}$  (Tab. 1). The same behaviour is observed for samples doped with  $\text{Eu}^{3+}$  ions. Then, the stability parameter  $\Delta T$  increases from 108 °C for IZBSEu up to 112 °C for IZBSGNEu. The thermal properties of IZBSGN glasses containing different concentrations of rare earth ions have been examined

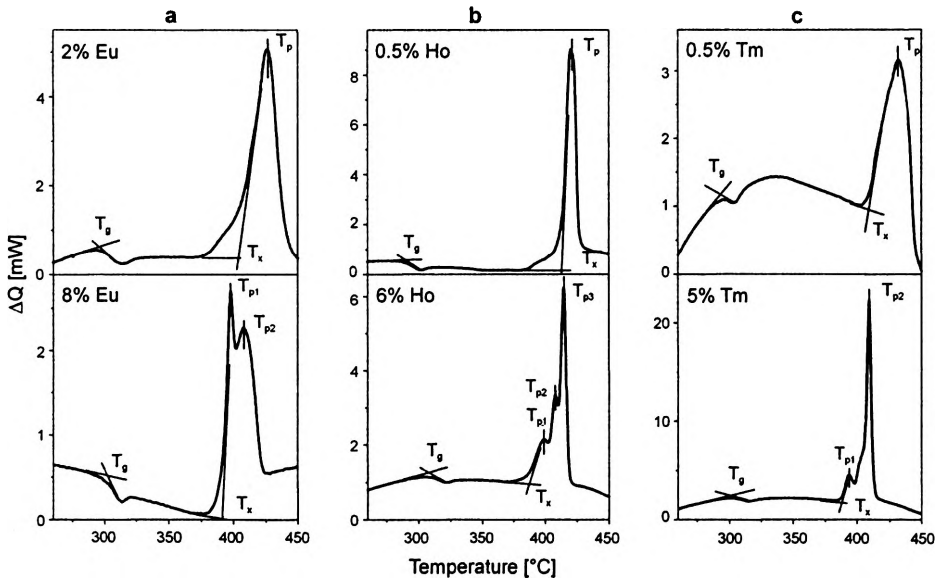


Fig. 2. DSC curves of  $\text{InF}_3$ -based glasses doped with  $\text{Eu}^{3+}$  (a),  $\text{Ho}^{3+}$  (b) and  $\text{Tm}^{3+}$  (c) ions.

T a b l e 3. Thermal properties of  $\text{InF}_3$ -based glasses doped with rare earth ions.

Ln-doped sample	$T_g$ [°C]	$T_x$ [°C]	$T_p$ [°C]	$\Delta T$ [°C]	$H$	$S$
2 mol% $\text{EuF}_3$	294	406	431	112	0.38	9.52
8 mol% $\text{EuF}_3$	307	389	398	82	0.27	2.40
0.5 mol% $\text{HoF}_3$	294	410	420	116	0.39	3.95
6 mol% $\text{HoF}_3$	306	386	399	80	0.26	3.40
0.5 mol% $\text{TmF}_3$	294	409	430	115	0.39	8.21
5 mol% $\text{TmF}_3$	300	388	394	88	0.29	1.76

(Fig. 2). The results are presented in Tab. 3. The thermal stability of the base glass has been found to increase upon the incorporation of no more than 2 mol% of rare earth ions. These results show that the addition of rare earth fluoride to the base glass lowers the crystallization rate and causes an increase in the thermal stability of the base glass. Adding above 5 mol% of rare earth fluoride causes an extremely strong decrease in the thermal stability parameter. It has been pointed out that our glass system, in which  $\text{GaF}_3$  and  $\text{NaF}$  were used as modifiers in  $\text{InF}_3$ -based glass doped with rare earth ions in the limit of low concentration, is more stable than the other one.

### 3.4. Optical study

Relaxation of excited states in the  $\text{InF}_3$ -based glasses containing different concentrations of  $\text{Eu}^{3+}$ ,  $\text{Ho}^{3+}$  and  $\text{Tm}^{3+}$  ions has been examined in our previous work [7]. Emission properties of these glasses doped with rare earth ions strongly depend on activator concentration. For higher activator concentration, strong luminescence quenching related to the contribution of activator–activator interaction by cross-relaxation processes is observed. Emission spectra and lifetimes of excited states give evidence that cross-relaxation processes are quite efficient in the  $\text{InF}_3$ -based glasses. From the optical absorption measurements and Judd–Ofelt method the intensity parameters have been obtained for rare earth ions in the  $\text{InF}_3$ -based glass. The trends of the Judd–Ofelt intensity parameters  $\Omega$  are examined as a function of the number of  $4f$  electrons. Figure 3 shows the variation of these parameters according to the rare earth series for  $\text{InF}_3$ -based glass. The parameter  $\Omega_2$  does not exceed  $2 \times 10^{-20} \text{ cm}^2$  for all rare earth ions in our glass system. The small values of parameter  $\Omega_2$  indicate that these glasses have a good chemical homogeneity [8] and are less covalent in character than the  $\text{ZrF}_4$ -based one [9]. The observed monotonous decrease in the intensity parameters  $\Omega_4$  and  $\Omega_6$  for rare earth ions in our glasses shows the dominant static mechanism of the Judd–Ofelt theory. In contrast to the crystalline materials, where  $\Omega_4$

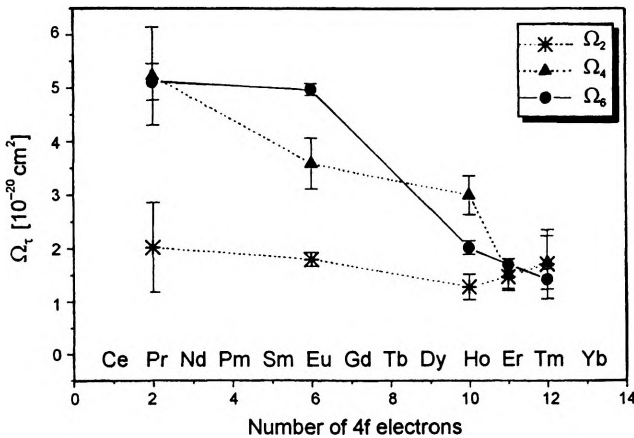


Fig. 3. Variation of the Judd–Ofelt intensity parameters  $\Omega_t$  ( $t = 2, 4, 6$ ) along the lanthanide series for the  $\text{InF}_3$ -based glass.

and  $\Omega_6$  values lie on a U-shaped curve [10] due to electron–phonon coupling, which is strong at the beginning and at the end of rare earth series [11], vibronic contributions to the transition intensities do not play an important role in the  $\text{InF}_3$ -based glass.

#### 4. Conclusions

The  $\text{InF}_3$ -based glasses have been obtained. In particular, glasses based on IZBSGN systems are more stable. Physical properties of these glasses using XRD, EPMA, DSC methods as well as optical absorption have been investigated. X-ray diffraction patterns do not reveal neither strong diffraction line due to the precipitation of  $\text{InF}_3$  nor other crystalline phases. Stability parameters were calculated basing on DSC measurements. The effect of  $(\text{GaF}_3, \text{NaF})/(\text{InF}_3, \text{BaF}_2)$  substitution and rare earth doping on thermal properties of  $\text{InF}_3$ -based glasses has been found. Stability parameter  $\Delta T$  increases with the addition of glass modifiers such as  $\text{GaF}_3$ ,  $\text{NaF}$ . In the limit of low activator concentration, thermal stability increases and the drastic decrease starts at higher concentration. The observed monotonous decrease in the parameters  $\Omega_4$  and  $\Omega_6$  from the  $\text{Pr}^{3+}$  ion to the  $\text{Tm}^{3+}$  ion shows that the vibronic contributions to the transition intensities in the  $\text{InF}_3$ -based glasses are not important. Additionally, small values of parameter  $\Omega_2$  suggest the high degree of homogeneity of these glasses, what was confirmed by EPMA results.

*Acknowledgments* – This work was supported by the Polish State Committee for Scientific Research (KBN) under grant No. 7 T08D 020 21.

#### References

- [1] POULAIN M., POULAIN M., *J. Non-Cryst. Solids* **213–214** (1997), 40.
- [2] DAKUI DONG, ZHONGLIN BO, JIQIAN ZHU, FUDING MA, *J. Non-Cryst. Solids* **204** (1996), 260.
- [3] MESSADDEQ Y., DELBEN A., BOSCOLO M., AEGERTER M.A., SOUFIANE A., POULAIN M., *J. Non-Cryst. Solids* **161** (1993), 210.
- [4] MESSADDEQ Y., INOUE S., RIBEIRO C.T.M., NUNES L.A.O., *J. Non-Cryst. Solids* **213–214** (1997), 179.
- [5] QIU J., MAEDA K., TERAI R., WAKABAYASHI H., *J. Non-Cryst. Solids* **213–214** (1997), 363.
- [6] RYBA-ROMANOWSKI W., GOŁĄB S., DOMINIĄK-DZIK G., ŻELECHOWER M., PISARSKA J., *J. Alloys Compd.* **325** (2001), 215.
- [7] GABRYŚ-PISARSKA J., ŻELECHOWER M., PISARSKI W.A., GOŁĄB S., BAŁUKA M., RYBA-ROMANOWSKI W., *Opt. Appl.* **30** (2000), 517.
- [8] REISFELD R., JORGENSEN C.K., *Excited state phenomena in vitreous materials*, [In] *Handbook on the Physics and Chemistry of Rare Earth*, Elsevier Science Publishers, 1987, Chap. 58.
- [9] TANABE S., *J. Non-Cryst. Solids* **259** (1999), 1.
- [10] PEACOCK R.D., *Str. Bonding* (Berlin) **22** (1975), 83.
- [11] MEIJERINK A., BLASSE G., SYTSMAN J., DE MELLO DONEGA C., ELLENS A., *Acta Phys. Pol. A* **90** (1996), 109.

*Received September 26, 2002*